A 3D printed beam splitter for polar neutral molecules

Sean D. S. Gordon[1] and Andreas Osterwalder[1, *]

[1]*Institute for Chemical Sciences and Engineering,*

Ecole Polytechnique Fédérale de Lausanne (EPFL), 1015 Lausanne, Switzerland

(Dated: November 8, 2016)

Supersonic molecular beams, obtained by expanding a gas from high pressure into vacuum, have been among the main tools in gas phase spectroscopy and reaction dynamics research for several decades.[1] A limit on experimental possibilities is imposed by weak and fluctuating signals, when small modifications of the beam composition need to be detected upon irradiation with light, or after collisions with another beam. Obtaining statistically significant data can require performing the experiment on a probe beam and then again on a reference beam – each of which can require a long averaging time. Here we demonstrate a device that permits probe and reference measurements to be performed simultaneously by splitting a single molecular beam into two correlated components with nearly identical properties. This arrangement substantially enhances the experimental sensitivity and paves the way to, e.g., studies of cold chemistry,[2–7] wherein the depletion of one beam-constituent can be recorded, rather than the formation of new products. Building upon experiments that use strong inhomogeneous electric fields to slow,[8–11] trap,[12–14] guide,[15–17] or merge[4, 18] polar neutral molecules,[7] our device uses such fields to spatially separate the molecular beam into two nearly identical components. The fields are produced through electric potential differences of several thousand volts between cylindrical electrodes a few mm apart.[19] Stringent quality requirements apply to the manufacturing of these electrodes because minute surface defects can lead to undesirable arcing. Traditional means of fabrication can provide good precision and surface finish, however they are limited in terms of the shapes which can be produced. Here, we 3D-print our setup in plastic and then electroplate to obtain atomically smooth metallic surfaces. The combination of 3D printing with electroplating represents a general method to produce electrically conductive, chemically robust structures with nearly any desired geometry.

―――――

*Electronic address: andreas.osterwalder@epfl.ch

Supersonic molecular beams provide high particle densities and low temperatures for gas phase chemical physics experiments, but these beams often suffer from pulse-to-pulse variations due to the mechanical properties of the pulsed valves. Suppression of statistical fluctuations can be achieved through sequential averaging of multiple uncorrelated events. This approach substantially improves the signal-to-noise ratio, but it is slow and can be vulnerable to long-term fluctuations in the experimental parameters. An alternative method is the real-time comparison of the probe signal with a correlated reference, the implementation of which we demonstrate here. We adapt a well-known concept used, e.g., in benchtop spectroscopy devices where a light beam is split into probe and reference, by dividing a single beam of neutral molecules into two correlated beams that retain their principal properties in terms of density and temperature. Here, polar molecules are collimated by an electrostatic hexapole guide that smoothly converts into two quadrupole guides. This setup paves the way towards differential measurements with unprecedented sensitivity and will allow, e.g., reactivity studies where rotational state specific reactivities are precisely map out by recording the depletion of their population in the probe beam relative to the reference. Density fluctuations in molecular beams currently render such experiments nearly impossible.

Macroscopic guides for polar molecules like ND_3 require very strong inhomogeneous electric fields which, through the Stark effect, generate a transverse confining force.[19, 20] These fields are produced through the application of large potential differences between specially shaped electrodes. For example, in the present experiment (see figure 1), the guide electrodes are cylindrical, placed at the vertices of a 6 mm hexagon, and have a diameter of 4 mm. The resulting gaps are 2 mm, and a potential difference of 20 kV across them produces a field of $\approx$100 kV/cm. A machining precision of better than 50 μm is essential, and the surface finish is critical for such devices: impurities, scratches, and similar defects on the electrode surfaces amplify the risk of electric arcing. For simple components this can be achieved by traditional precision machining, but the bent and split shape of the electrodes required here to transform the hexapole guide into quadrupole guides is nearly impossible to make by traditional means. To produce a device that fulfils the mechanical, geometric, and electrical criteria, we apply a modern production method, namely the 3D printing of the entire electrode structure as a single plastic piece. The piece is then selectively electroplated with a metal layer $\approx$10 μm thick . The metal plating not only allows the almost free choice of surface material, including some that would be very hard to machine, it also produces a surface quality superior to that obtained through mechanical polishing.

The simple and powerful fabrication method introduced here opens a plethora of new avenues for research, far beyond molecular beams experiments, since 3D printing imposes practically no limitations on possible shapes, and
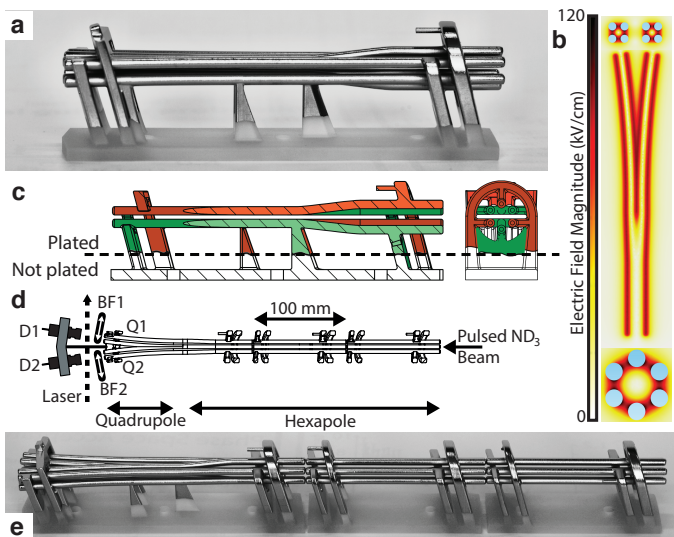
FIG. 1: a: the 3D printed and selectively electroplated beam splitter. Molecules enter from the right and are first confined in an hexapole (see bottom of panel b) which smoothly converts into two quadrupoles (top of panel b). The central part of panel b shows the electric field magnitude in the device as a top-view. c: Cross section through the beam splitter. Red and green designate two regions of differing voltages that need to be electrically isolated from one another. d: guide and detector arrangement. The ND_3 beam traverses the guide from right to left. A laser beam crosses the molecular beams behind the guide structure to ionise molecules emerging from guides Q1 and Q2. Detectors D1 and D2 record signals from each of the guides individually. Guides can be blocked by retractable beam flags BF1 or BF2. The complete guide assembly where the beam splitter is proceeded by two straight hexapoles is shown in panel e.

the metal-plating produces chemically robust, conductive construction elements. It has the added advantage of dramatically reduced production cost and time: all components used in the present study were printed within less than 48 hours; electroplating is completed in one day, and the bottle neck of the entire process was the shipping to and from the plating company. This dramatic acceleration in comparison with traditional manufacturing which, for such pieces, can require months and produce lower quality results, allows for a very fast turnover and more flexibility in the development and testing of new components. Furthermore, the entirely digital workflow has the advantage that an inherently exact replica of a complete experimental setup can be produced in any laboratory, simply by transferring a small file, and making use of local production infrastructure.

Our beam splitter is shown in figures 1a and c. The complete structure, two straight guides plus beam splitter, is displayed in figure 1e (for a detailed description of the experiment and stereolithography files of all elements, see the supplementary material). Panel d shows the experimental arrangement, which is entirely housed inside a high-vacuum chamber. A pulsed beam of ND_3 is fed into the guide from the right. Two separate beams are formed where
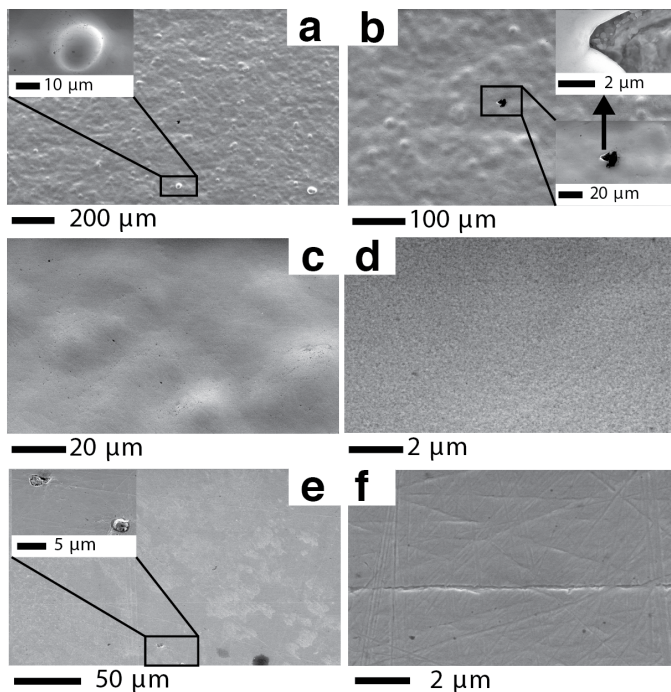
FIG. 2: Scanning Electron Micrographs of metal plated, 3D-printed PMMA (panels a-d) and of highly polished stainless steel (e and f).

the hexapole splits into quadrupoles, and molecules are detected individually on separate detectors behind each of the guides. A single pulsed laser beam crosses both molecular beams and ionises the ND_3 by rotationally resolved resonance-enhanced multi-photon ionisation (REMPI).[17, 21]

Figure 1b provides a top-view of the electric field distribution inside the beam splitter. The single electric field minimum that confines the ND_3 molecules in the hexapole (bottom) is converted into two field minima in the quadrupoles (top). The structure in figure 1a was produced as a single piece made from poly(methyl methacrylate) (PMMA) by means of stereolithography. In order to generate fields as in figure 1b the electrodes must be held at alternating dc-voltages. We achieve this by using a structure that enables the electrical isolation of the electrode groups, as shown in figure 1c. The supports to the left and the right are holding one set of electrodes each, indicated by the color coding in figure 1c. The central supports hold a single electrode each to ensure mechanical rigidity during printing.

Electrical conductivity is obtained by coating certain regions, shown as red and green areas in figure 1c, of the PMMA piece with a nickel layer. Directly 3D printing a metal piece is possible but yields a lower surface-quality. Non-conductive polymers can be printed at precisions around 20 μm on benchtop devices, and plating through a combination of chemical and electrolytical procedures (performed by Galvotec GmbH, Switzerland[22]) produces the high quality surfaces required for the stable production of strong electric fields. Sharp edges or material protrusions
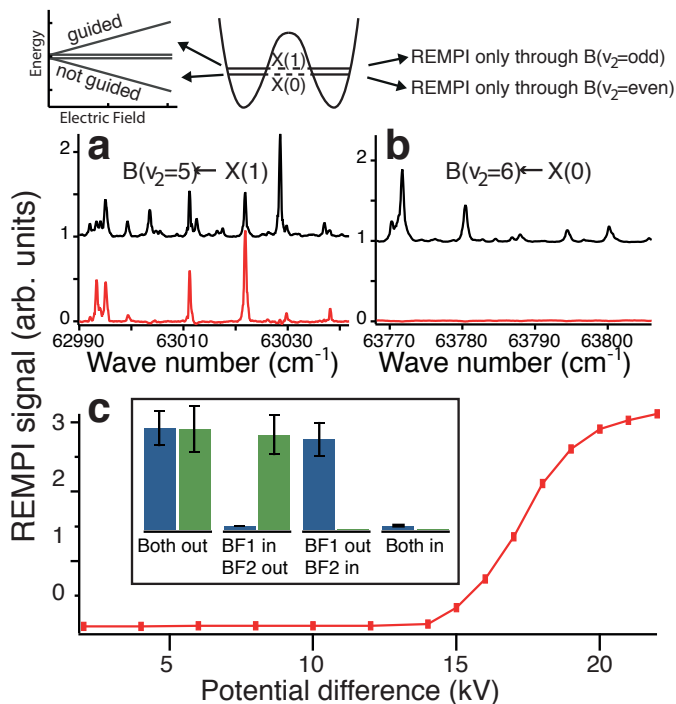
FIG. 3: a and b: REMPI spectra recorded through the B(ν_2=5) and B(ν_2=6) vibronic levels, respectively. Black (red) traces show the signal of the pure (guided) molecular beam. A schematic explanation of the relevant physics is given above the panels (see text). c: Signal as a function of the voltage difference between positive and negative electrodes. The inset shows the signals on the two detectors when beam flags are selectively blocking none, one, or both beams.

lead to very strong local electric field enhancements which in turn promote arcing.[23] The surface properties of our printed pieces are characterised here by electron microscopy. Figure 2 shows the surface of a 3D printed, metal-coated piece (panels a-d) and of a mechanically polished stainless steel piece for comparison (panels e and f). The electroplated piece is not perfectly flat and reveals minor defects (panels a and b), but the majority of the surface is devoid of edges and protrusions. Defects are either rounded and relatively large bumps on the surface, as shown in the inset in panel a, that do not dramatically alter the electric field distribution, or they resemble the cavity shown in the inset of panel b, leading to protected pockets. Both forms of defect do not strongly provoke arcing.[23] For the most part, the surfaces are atomically smooth (panels c and d), which ensures very good electrical performance in strong electric fields. In contrast, the highly polished stainless steel piece shown in panels e and f is flat but shows scratches at a nm scale that ultimately limit the performance in strong electric fields.

The principal results of our study are collected in figures 3 and 4. Panels 3a and b demonstrate spectroscopically that we detect guided molecules, showing the REMPI signals recorded for the molecular beam without (black traces) and with guiding (red traces). The sketch above the spectra explains the physics behind this measurement, an
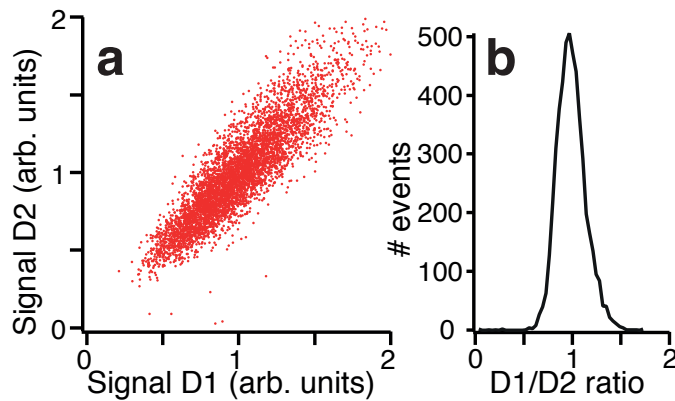
FIG. 4: a: Correlation between the normalised signals recorded on detectors D1 and D2. Each point represents one measurement. b: Histogram of the ratio between the D1 and D2 signals. The correlation coefficient for the data in a is 0.89, and standard deviation of the distribution in b is 15%.

unambiguous confirmation that we indeed record guided molecules rather than the direct molecular beam: of the two components of the inversion doublet in ND_3 only the upper level can be guided and, due to spectroscopic selection rules, it can only be detected via $B(\nu_2=odd)$ vibronic levels. In contrast, the lower component is not guided and can only be detected through $B(\nu_2=even)$ levels (see supplementary material for details). Several transitions from low rotational states in the original molecular beam are observed in the original beam. In contrast, only transitions from guided states are visible in the red traces, thus dramatically simplifying the spectrum in 3a and reducing that in 3b to pure background.

To bend the ND_3 beam in a curved guide, a minimum electric field is required that compensates for the centrifugal force.[24] In figure 3d the potential difference on the guide electrodes is gradually increased to 22 kV. The curve reveals the electric field magnitude required to efficiently compensate for the centrifugal force in the curved quadrupole section and guide the molecules to the detectors: the forward velocity of several 100 m/s from the initial expansion requires a field of almost 100 kV/cm (corresponding to a potential difference of 20 kV) to bend the ND_3 beam around the 6 m-radius used here. The inset in figure 3d shows the signal on detectors D1 and D2 when the beams from Q1 and Q2 are selectively blocked by retractable beam flags and provides another confirmation for the detection of molecules from the beam.

Differential measurements require a correlation between probe and reference signals. In figure 4a the simultaneously measured, normalised signal intensities from 5000 single-pulse measurements on detectors D1 and D2 are plotted against each other. Both signals individually fluctuate, due to shot-to-shot variations of density and detection laser, however there is a clear correlation, and all data points lie near the 45-degree diagonal. The histogram of the D1/D2

signal ratio shown in figure 4b has a standard deviation of 15%, and analysis of the data in figure 4a gives a correlation coefficient of r=0.89. Correlated molecular beams will now be used to perform new classes of experiments wherein the composition of the probe beam is continuously monitored relative to the reference beam. This enables, e.g., dynamics experiments with highly accurate determination of rotational state specific reactivities. Rotating a beam splitter by 180 degrees, and injecting two separate supersonic expansions, will enable the merging of two molecular beams and allow the first low-temperature reactivity studies between two polar reactants.[4, 18]

I. ACKNOWLEDGMENTS

II. AUTHOR CONTRIBUTIONS

AO devised and designed the experiment. SDSG and AO jointly performed the experiment and wrote the manuscript.

[1] G. Scoles, *Atomic and Molecular Beam Methods.* (Oxford University Press, 1988).

[2] D. W. Chandler, J. Chem. Phys. **132**, 110901 (2010).

[3] M. Brouard, D. H. Parker, and S. van de Meerakker, Chem. Soc. Rev. **43**, 7279 (2014).

[4] A. Osterwalder, EPJ Techniques and Instrumentation **2**, 10 (2015).

[5] J. Jankunas and A. Osterwalder, Annu. Rev. Phys. Chem. **66**, 241 (2015).

[6] B. K. Stuhl, M. T. Hummon, and J. Ye, Annu. Rev. Phys. Chem. **65**, 501 (2014).

[7] D. Jin and J. Ye, *Special Issue on Ultracold Molecules*, vol. 112 (Chemical Reviews, ACS Publications, 2012).

[8] H. L. Bethlem, G. Berden, and G. Meijer, Phys. Rev. Lett. **83**, 1558 (1999).

[9] E. R. Hudson, J. Bochinski, H. Lewandowski, B. C. Sawyer, and J. Ye, Eur. Phys. J. D **31**, 351 (2004).

[10] L. Scharfenberg, H. Haak, G. Meijer, and S. van de Meerakker, Phys. Rev. A **79**, 023410 (2009).

[11] A. Osterwalder, S. A. Meek, H. Haak, and G. Meijer, Phys. Rev. A **81**, 051401 (2010).

[12] H. L. Bethlem, G. Berden, F. Crompvoets, R. T. Jongma, A. Van Roij, and G. Meijer, Nat. Chem. **406**, 491 (2000).

[13] S. van de Meerakker, P. Smeets, N. Vanhaecke, R. T. Jongma, and G. Meijer, Phys. Rev. Lett. **94**, 023004 (2005).

[14] B. C. Sawyer, B. K. Stuhl, M. Yeo, T. V. Tscherbul, M. T. Hummon, Y. Xia, J. Kłos, D. Patterson, J. M. Doyle, and J. Ye, Phys. Chem. Chem. Phys. **13**, 19059 (2011).

[15] S. Chervenkov, X. Wu, J. Bayerl, A. Rohlfes, T. Gantner, M. Zeppenfeld, and G. Rempe, Phys. Rev. Lett. **112**, 013001 (2014).

[16] S. A. Rangwala, T. Junglen, T. Rieger, P. W. H. Pinkse, and G. Rempe, Phys. Rev. A **67**, 043406 (2003).

[17] B. Bertsche and A. Osterwalder, Physical Review A **82**, 033418 (2010).

[18] A. B. Henson, S. Gersten, Y. Shagam, J. Narevicius, and E. Narevicius, Science **338**, 234 (2012).

[19] S. van de Meerakker, H. L. Bethlem, N. Vanhaecke, and G. Meijer, Chem. Rev. **112**, 4828 (2012).

[20] S. van de Meerakker, H. L. Bethlem, and G. Meijer, Nat Phys **4**, 595 (2008).

[21] M. N. R. Ashfold, S. R. Langford, R. A. Morgan, A. J. Orr-Ewing, C. M. Western, C. R. Scheper, and A. de Lange, Eur. Phys. J. D **4**, 189 (1998).

[22] *Galvotec GmbH, Switzerland*, URL `http://www.galvotec.ch`.

[23] R. Latham, *High Voltage Vacuum Insulation*, Basic Concepts and Technological Practice (Academic Press, 2001).

[24] T. Junglen, T. Rieger, S. A. Rangwala, P. W. H. Pinkse, and G. Rempe, Eur. Phys. J. D **31**, 365 (2004).